This article has been accepted for publication in a future issue of this journal, but has not been fully edited. Content may change prior to final publication. Citation information: DOI 10.1109/JSEN.2016.2627798, IEEE Sensors Journal

Towards Bio-inspired Tactile Sensing Capsule Endoscopy for Detection of Submucosal Tumours

B Winstone*, $CMelhuish^*$, $TPipe^*$, $MCallaway^+$, $SDogramadzi^*$

***Abstract*—Here we present a method for lump characterisation using a bio-inspired remote tactile sensing capsule endoscopy system. Whilst current capsule endoscopy utilises cameras to diagnose lesions on the surface of the gastrointestinal tract lumen, this proposal uses remote palpation to stimulate a bio-inspired tactile sensing surface that deforms under the impression of both hard and soft raised objects. Current capsule endoscopy utilises cameras to visually diagnose lesions on the surface of the gastrointestinal tract. Our approach introduces remote palpation by deploying a bio-inspired tactile sensor that deforms when pressed against soft or hard lumps. This can enhance visual inspection of lesions and provide more information about the structure of the lesions. Using classifier systems we have shown that lumps of different size, shape and hardness can be distinguished in a synthetic test environment. This is a promising early start towards achieving a remote palpation system used inside the GI tract that will utilise the clinician's sense of touch.**

***Keywords*—Tactile sensing, Capsule endoscopy, Remote palpation, Tumour classification**

I. Introduction

Inspection of gastrointestinal tract and minimally invasive surgeries where long slender instruments are introduced in the human body for diagnostic and therapeutic purposes, although clinically increasingly important, do not allow the surgeon to directly palpate the tissue. This problem has been the subject of many research groups, particularly in the integration of haptic feedback to Robot Assisted Minimally Invasive Surgery (RAMIS) to aid in guidance and diagnostics. Trejos et al. [1] show that tactile sensing RAMIS procedures reduce applied maximum force in the tissue by more than 35% compared to manual palpation. In 2006 Schostek et al. [2] presented work on adding tactile sensing capabilities through visual feedback to laparoscopic manipulation without tactile sensing in order to aid in local tumour surgery. More recently in 2013 Roke et al. [3] took this concept further with the addition of a tactile feedback display using a mechanical matrix of linear actuators to remotely stimulate the operators fingers based on sensor deformation in contact with artificial tissue and tumours. Gwilliam et al. [4] further support evidence presented by Sarvazyan et al. [5] that computerised or electronic palpation can be more effective at detecting lumps than the human finger.

In the work of Menciassi et al. [6] list the main challenges of endoscopes being their limited degree freedom, and more importantly lack of sensing capability which presents major risk of excessive force application. Dogramadzi et al. [7] have presented a method to measure in vitro colonoscope forces along the length of the shaft, Rebello [8] discusses endoscopic tips with contact, force and pressure micro-sensors to aid in user feedback. In 2011 Kume et al. [9] investigated the development of an articulated robotic endoscopic tool. Although adding articulation showed evidence that the insertion becomes easier, and learning to operate quicker, they clearly state that tactile feedback would aid in limiting excessive application of force. Further evidence of the lack of, but need for tactile sensing in remote surgical systems is discussed by Chaudhary et al. [10] in their review of medical robotics. The capsule endoscopy introduced by Given Imaging PillCam brought a novel approach to gastrointestinal diagnostics but not without limitations. The capsule is propelled by peristalsis and its motion can not be controlled. Further research on improving its abilities have been made on traversing the entire abdominal environment to perform biopsy of hepatic tissue with a mobile in vivo camera robot, [11], simple controlled observation of the GI tract, [12] [13] or drug deliver, [14].

One of surgeon's most important skills is their highly enhanced sense of touch [15]. Minimally invasive approaches to diagnostics in medical technology often restricts direct palpation of the patient. Whilst systems for laparoscopic surgery introduce minimally invasive procedures that minimise patient discomfort and improve recovery, they are making much less use of this very human perception. Direct contact sensing has long been a common practice for diagnosis in the vast majority of medical fields. Cox et al. [15] present the reason that we palpate the skin, it not only presents reassurance to the patient but more importantly, it is an underestimated examination modalitity that identifies tenderness, consistency, induration, depth and fixation. Palpation is used to identify strained muscles, skeletal breaks and deformed growths amongst other signs of ill health.

Konstantinova et al. [16] have reviewed the latest developments in tactile sensors for robot assisted minimally invasive surgery with a focus on manual palpation. They state that "*Nowadays, no sensor system exists that is capable of accurately measuring the full complexity of tactile cues on the same level as the human tactile receptive system*", emphasising that this is a needed development for accurate perception in robot assisted medical procedures. In 2004 Dargahi et al.'s [17] review discusses the importance of modelling human tactile perception as a standard in the development of tactile sensing systems.

Other examples of remote palpation using tactile sensors can

* B Winstone, S Dogramadzi, C Melhuish T Pipe are with the Bristol Robotics Laboratory, University of the West of England, Bristol, UK. benjamin.Winstone@brl.ac.uk

+ M Callaway is with the Department of Radiology, Bristol Royal Infirmary, Bristol, UK.

be found in [18] where the detection of stiff nodules beneath soft tissue is achieved using a resonance sensor. The system is able to detect stiffness changes at least 4 mm away from the biological specimen. Nyberg et al [19] combine Raman spectroscopy with tactile resonance technology to achieve discrimination of normal prostate tissue ex vivo. Using stepwise analysis to combine system parameters they achieved 100% sensitivity, with a 91% specificity for discriminating non-epithelial and epithelial tissue. Finally, Chuang et al [20] utilize a tactile sensor with structural electrodes for differentiating the mechanical properties of elastomeric materials. The presented sensor is suitable for mounting on an endoscope for the hardness detection of submucosal tumors. Further work can also be seen using haptic feedback as a means to relay remote tactile sensing. Talasaz et al presents force feedback stimulated by a capacitive tactile sensor mounted to a laparoscopic tool [21], and Tanaka et al, [22] have used a voice coil based tactile array to stimulate the finger with data acquired from a tactile sensor also located on a laparoscopic tool.

Although examples can be found in the scientific literature of technology capable of tactile palpation of the external surfaces of the body or internally through a limited reach tethered system, Ciuti et al. [23] review the frontiers of robotic endoscopic capsules and report that no work has yet focused on remote palpation using an untethered capsule for examination of the GI tract. Capsule endoscopy (CE) utilises a swallowable capsule with a self contained microsystem, similar to a traditional drug delivery capsule. CE provides a platform to achieve similar procedures to more traditional methods of endoscopy but without the difficult and time consuming insertion of an endoscope. This presents a capability to explore the entire length of the GI tract including the small intestines which is not currently possible using any other system. In its current form capsule endoscopy is limited to only visual inspection of the lumen surface. Tissue health deeper than the lumen surface cannot be detected by visual means, however using a tactile palpation technique deep tissue deformities could be sensed.

Modern capsule endoscopy presents an ability to view the small bowel beyond the duodenum and proximal to the colon. There are a number of pathologies that can occur in the small bowel, such as tumours, strictures and ulceration as part of an inflammatory bowel condition such as crohns disease. Shi et al. [24] discusses the importance of the GI tract motility and how failings in motility can be an indication of more serious GI diseases. Shi presents a sensing capsule to measure pressures encountered during the journey through the GI tract as an indication of GI tract motility. The capsule robot sensor presented in this paper would be suitable to detect GI tract motility through measuring the deformation of the capsule walls due to forces exerted by GI tract action. As the capsule sensor passes through the GI tract, a map of tract motility can be recorded.

In this paper we utilize a biomimetic tactile fingertip technology, the Tactip, to create a biologically inspired system capable of remote operated palpation with a 6-axis arm to provide localisation and characterisation of bowel lining beyond what is typically identifiable through vision alone. Building on the recent work showing capabilities of this design [25], we investigate the suitability of the sensor for use with a classifier system to discriminate shape, size and softness of bowel deformities. This will not only demonstrate a suitability for remote palpation and tactile sensing but also a step towards an automated diagnostics system. Using a tactile sensing system that is based on the human finger sensing anatomy could provide a new diagnostic technique not yet explored. This paper focuses on acquisition of tactile sensing data that closely matches the form of human tactile stimulus, it is considered that this form is highly suitable for haptic systems. Future work will match this sensing data with a suitable tactile haptic feedback device to create a closed loop remote haptic sensing technology. Furthermore it is assumed that it would later be integrated with an untethered locomotion system for active exploration to enable a complete remote sensing technology to the surgeon.

II. Biologically-inspired tactile sensing device

The Tactip is a biologically-inspired sensing technology, based upon the deformation of the epidermal layers of the human skin. Deformation from device-object interaction is measured optically by tracking the movement of internal papillae pins on the inside of the device skin. These papillae pins are representative of the intermediate epidermal ridges of the skin, whose static and dynamic displacement are normally detected through the skin's mechanoreceptors, see Fig. 1. In past publications we have shown how the Tactip can be used for edge detection [26], lump detection [3] [27] and texture discrimination [27]. In this paper we have adapted the principles of the Tactip to fit the form of a capsule endoscope, developing a pill like capsule based upon the human biological model of tactile sensing that is capable of lump detection. The advantage of using the Tactip sensing technology over a sensor that is not deformable is that its compliancy works in favour of the GI tract environment. A non-deformable sensor will more likely cause blockage whilst a soft sensor can deform to its surroundings whilst still sensing. This could avoid obstruction of the peristaltic flow of the GI tract whilst moving with or against the flow of the gut.

In its current form the cylindrical Tactip can be compressed by $7mm$ from any direction, or $14mm$ from opposing directions, before the internal papillae pins collide with internal acrylic tube. As part of future miniaturisation this compressibility could be increased if the camera system space occupancy is reduced, allowing a reduction in the diameter of the acrylic tube. Additionally, a flexible internal tube could be used instead of the acrylic tube, to further increase compliance with external compressive forces. The forces required to compress the cylindrical Tactip are presented later in Fig. 11, where the cylindrical Tactip has been measured up to $8N$, however, Kamba et al. [28] identified human stomach compression forces up to $1.9N$. In previous work [29], it has been shown that changing materials for the skin increases compliance and sensitivity of the Tactip device. The design presented is subjected to the properties available from the Object 260 3D rubber printer and tango black plus material. However,

This article has been accepted for publication in a future issue of this journal, but has not been fully edited. Content may change prior to final publication. Citation information: DOI 10.1109/JSEN.2016.2627798, IEEE Sensors Journal

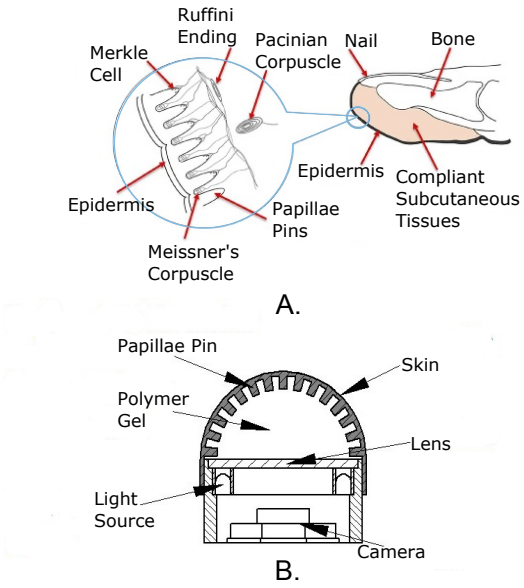

Fig. 1. Tactip concept, A. biological model and B. engineered model.

it is very feasible that using more compliant materials the cylindrical Tactip would be more easily compressible to suit the weaker forces of the GI tract.

There are two mechanoreceptors in particular that respond to the type of tactile interaction that this paper explores, the Meissner corpuscle and the Merkel cell [30]. The Meissner corpuscles adapts quickly to when stimulus is both applied and removed, and so are sensitive to movement across the skin. They are sited at the base of and between surrounding papillae. Any changes in distance between papillae will be detected by the Meissner corpuscle. The Merkel cell is sensitive to light touch, responding to the shape of the contacting surface. Merkel cells are sited at very specific locations on the tips of the dermal papillae, see Fig 1.A, where they are stimulated by the papillae tip movement. The Tactip system mimics this tactile sensing system by visually tracking the papillae movement as if it were the described mechanoreceptors.

Fig. 1 shows the design of a traditional Tactip concept which comprises an artificial cast silicone skin, optically clear flesh like gel, camera and internal illumination using LEDs. Whilst in the biological model it is the papillae pin movement that stimulates the mechanoreceptors in the finger, the Tactip design replaces the mechanoreceptor for a camera system capable of tracking pin interaction visually. Through the use of 3D printing technology it has been possible to develop a cylindrical form of the Tactip which can sense 360^o around the central axis. Using an Objet Connex 260 printer which prints hard and soft materials simultaneously, this new Tactip is printed in one process. The quality and robustness of such printed material is not yet as good as a cast rubber silicone which has been used previously, however for the purpose of experimentation it greatly speeds up the whole development process. Complete assembly only includes fitting the internal clear acrylic tube, casting the flesh like gel and fitting the

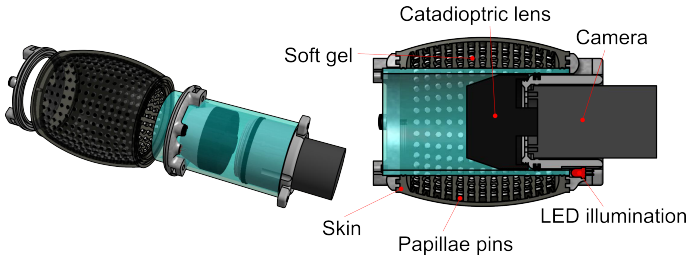

Fig. 2. Exploded and Cross section view of cylindrical Tactip pill design.

camera and catadioptric mirror system that is capable of a observing 360^o field of view. Fig. 2 presents an exploded view of the cylindrical Tactip, left, and cross section of the cylindrical Tactip design, right. As with a traditional Tactip design, it comprises an artificial 3D printed skin, optically clear flesh like gel, camera and internal illumination, but in addition uses a catadioptric mirrored lens. The camera used is a Microsoft LifeCam Cinema HD.

The internal view through the catadioptric mirror occupies $406 * 406$ of the $720 * 1200$ resolution camera view. The 360^o degree view is presented as a ring which is later unwrapped in to a 2D representation, see Fig. 3. Axial movement of pins has a relationship of 1 pixel to 0.24 mm, whilst radial movement is more complicated. If we consider the middle row of pins, they are situated within a circumference of 946 pixels. This determines the minimum pin movement that can be detected radially. The outer diameter of the device at the point of this middle row is 63 mm, whilst the tip of the papillae form a diameter of 54 mm, and circumference of 201 mm. This determines that one pixel covers 0.21 mm. The inner row has a smaller physical circumference of 167.5 mm, and pixel circumference of 726 pixel, providing a relationship of 1 pixel to 0.23 mm. Finally the outer row has a physical circumference of 167.7 mm, pixel circumference of 1165 and relationship of 1 pixel to 0.14 mm. The catadioptric mirror has produced a system that provides greater sensitivity to certain areas than others, and the rounded shape of the Tactip further distorts this perspective. Whilst this current model is larger than a typical capsule endoscopy pill, it's miniaturisation is achievable. In this case the restricting factor is the size of the catadioptric mirror system where one-off custom mirrors are expensive. Mass production would remove this cost to achieve a much smaller mirror system, and accompanying electronics can be miniaturised. All other components are easily miniatured such as the camera, which is evidence in current capsule endoscopes, and materials which have already undergone considerable reduction in [29] & [31] where reduced models suffered no loss in sensitivity.

Recent work by Winstone et al. [25] has shown active sensing ability of the capsule Tactip to detect surface deformation of various lumps associated with suspect tissue that could reside within the GI tract. Using a 6-axis robot arm, the capsule Tactip was fed through 74mm internal diameter acrylic tube with six artificial lumps placed randomly along a length of 250mm, see Fig. 4. The lumps varied in size

This article has been accepted for publication in a future issue of this journal, but has not been fully edited. Content may change prior to final publication. Citation information: DOI 10.1109/JSEN.2016.2627798, IEEE Sensors Journal

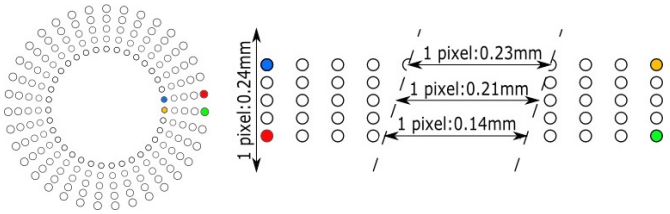

Fig. 3. Left: Diagram showing pin orientations from raw image before unwrapping. Right: Diagram showing pin orientations from unwrapped image and relative pixel to distance ratio for radial and axial movement.

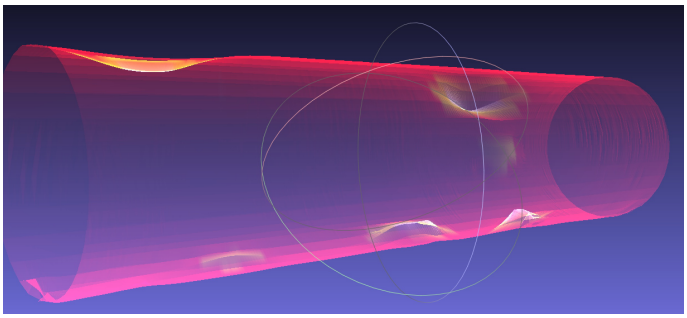

Fig. 5. 3D reconstruction of test environment built from data captured by the cylindrical Tactip sensor.

and material where differences can be seen in the sensor readings. Data was captured at 1mm increments along the length of the tube and reconstructed as a 3D rendering, see Fig. 5. By using different size lumps with different density materials it has given an indication of whether the Tactip capsule can distinguish between different types of deformation where a more complex algorithm could detect different feature characteristics, such as shape, size and softness.

In this report it is hypothesised that typical submucosal tumour like lumps found growing circumferentially around the lumen can be detected and classified using the Tactip capsule device.

III. Experiment Design

A. Experiment environment

The experiment environment comprises of four components, a cylindrical Tactip, a six axis ABB IRB120 robot arm, a 74mm internal diameter acrylic tube and a solid or soft test lump placed in a known location within the tube. Tumours differ in physical properties depending on their type and location on the body. A number of different approaches have been used when creating simulated tumours, from [32] that use 3 mm synthetic tumours ranging from shore 30 A to 60 A to [33] who have used a tumour made from shore 70 A. Submucosal tumours spread circumferentially around the lumen as the size increased. In these experiments, two types of synthetic tumours are used, a soft silicone cast shore 15 A and hard verowhite shore 85. These values fit in line with other research approaches, whilst presenting the opportunity to discriminate between different tissue density.

The robot arm is used during this experiment as a mode of locomotion for the capsule. The future vision is that the capsule would be capable of untethered locomotion through the GI tract with the addition of an appropriate locomotion system, however current work focuses purely on the tactile sensing capabilities. In order to collect a large sample set and test the full circumference of the sensing surface, the Tactip is pushed in 1mm increments along a 70mm length of the tube for complete coverage of the lump and then rotated by 10 degrees for the next scan, so that a total of 36 scans of the 70mm length are made for each test lump providing 2520 trial images. At each position within the tube 36 samples are taken, which will prove repeatability of the sensor if results match. At each instance an image is grabbed from the camera through the catadioptric lens which captures a 360 degree view, it is then translated into a two dimensional image. The image is further processed before sensor data can be acquired.

In this experiment the sensor is moved with specific increments in order to collect a sufficient sample set for the classifier. The real world application would see the sensor traverse through the lumen either propelled by the peristaltic contractions of the gut, or a future developed locomotion system attached to the sensor. The sampling frequency will be restriction by the frame rate of the camera, and processing time of the algorithm. [34] have studied gastrointestinal transit velocity, where fast velocity is considered to be 15cm / minute. If the Tactip was to sample at a minimum of once per mm, then a frame rate of 2.5 fps would achieve this. If a locomotion system was to guide the Tactip through the gut, then an increased speed would demand a higher frame rate.

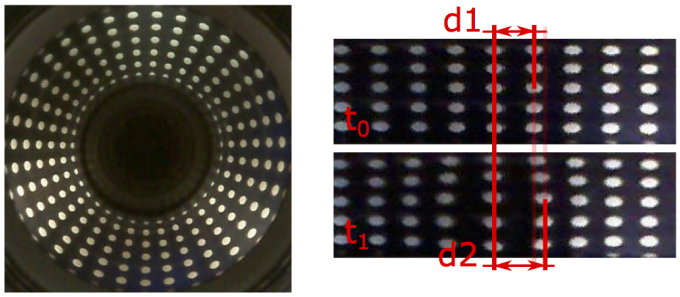

Fig. 6. Raw camera image showing calibration state on the left t_0, and post unwrapping of image, contact with lump state t_n on the right highlighting the location of the contact. d1 is the calibrated distance between pins before any external contact, d2 shows a new larger distance between pins at the focal point of contact. Pin displacement typically remains under 30 pixels per pin, which is approximately 6 mm physical distance.

B. Sensing algorithm

The algorithm used to interpret tactile interaction with the capsule focuses on papillae pin movement replicating the role of the Meissner's corpuscle and Merkel cell mechanoreceptors in the human finger. When objects contact the deformable capsule skin, pins within the region of contact separate from each other whilst neighbouring pins move closer to each other. This can be seen in Fig. 6 where the first image shows the

This article has been accepted for publication in a future issue of this journal, but has not been fully edited. Content may change prior to final publication. Citation information: DOI 10.1109/JSEN.2016.2627798, IEEE Sensors Journal

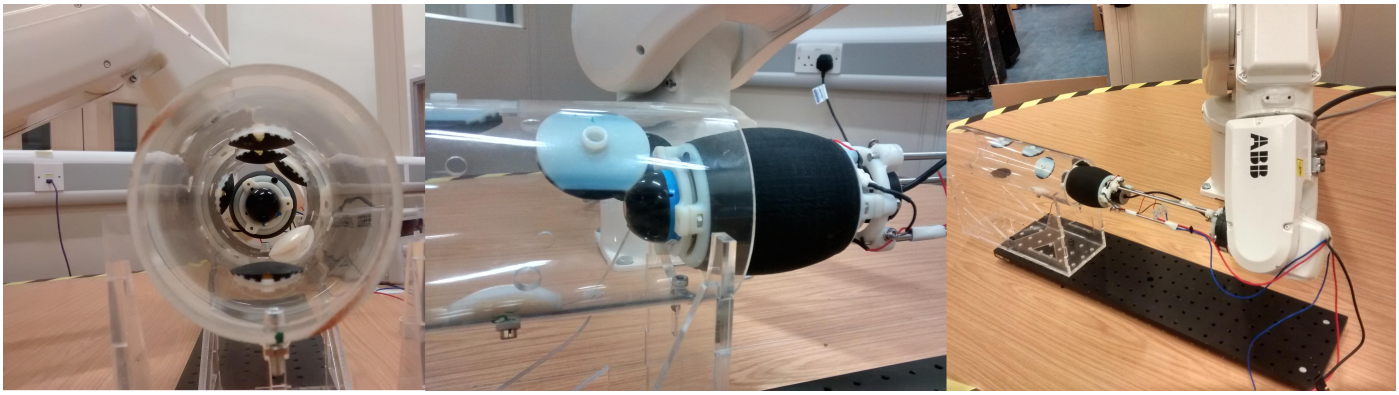

Fig. 4. Experiment setup, ABB IR120 pushing tactile sensing through rigid tube containing raised lumps.

Tactip in a relaxed state with no objects in contact with the skin, whilst the second image shows the Tactip in contact with a lump highlighted by d2 where the papillae pins have separated in the region of contact. The first stage of image processing is unwrapping the distorted 360^o image using the algorithm described in Equation 1 which shows how to calculate the corresponding pixel in the source image to the destination image.

$$d(x,y) = s((cos(x*(2\pi/W))*y)+R, (sin(x*(2\pi/W))*y)+R) \quad (1)$$

s = 360 source square image array
R = Radius of 360 image
W = Width of destination image
d = Destination flat image W * R
x = Horizontal pixel co-ordinate
y = Vertical pixel co-ordinate

After iterating through the source image using Equation 1, a two dimensional image is created with the papillae arranged in a grid formation. Using the OpenCV feature detection library papillae pin positions can be tracked and compared to previous states. In order to identify the location of deformation or lump contact, pin locations are compared against the relaxed calibrated state. In particular it is the increase in pin separation that highlights the location of skin deformation, so pixel distance between pins is used as the measurement value. Fig. 7 shows a matrix of vectors that represent the movement of each pin when pressed against a lump. The apex of the lump is noted by the region surrounded by vectors oriented away in all directions. This flow of vectors extends to the area of contact with the lump.

Gaps between pins that exceed the calibrated state provide a representative value of deformation at that location. Fig. 8 shows a localised group of pins subjected to skin contact where the pins within the contact region separate and the adjacent neighbouring pins move towards each other. It is these pin location deviations from calibrated state that form the input data to a classifier system. Encoded within the list of pin positions are the deformation features of the skin.

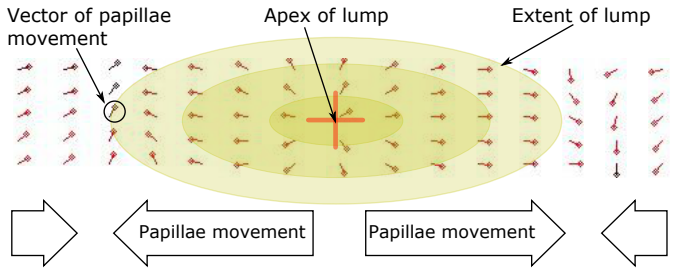

Fig. 7. Representation of difference in pin position with vectors. Location of lump is inferred through the centre of vector activity. The extent of the lump contact is inferred by the boundaries of vector flow.

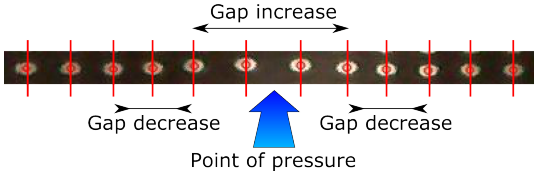

Fig. 8. Localised group of pins subjected to skin contact showing the pins within the contact region separate.

The delta value of pin position can be represented visually as shown in Fig. 9. In this figure examples of contact with each of the three lump sizes are shown and the source image is placed above the processed image. The delta value of each pin's movement is used as a colour intensity parameter for each cell in the grid. Additionally the vector angle is presented with the line and marker. This shows the typical differences between lump sizes and how only a small amount of movement of the pins can easily be detected through the camera.

C. Classifier systems

A Support Vector Machine (SVM) is a supervised learning model discriminative classifier, formally defined by a separating hyperplane, used for classification and regression analysis.

This article has been accepted for publication in a future issue of this journal, but has not been fully edited. Content may change prior to final publication. Citation information: DOI 10.1109/JSEN.2016.2627798, IEEE Sensors Journal

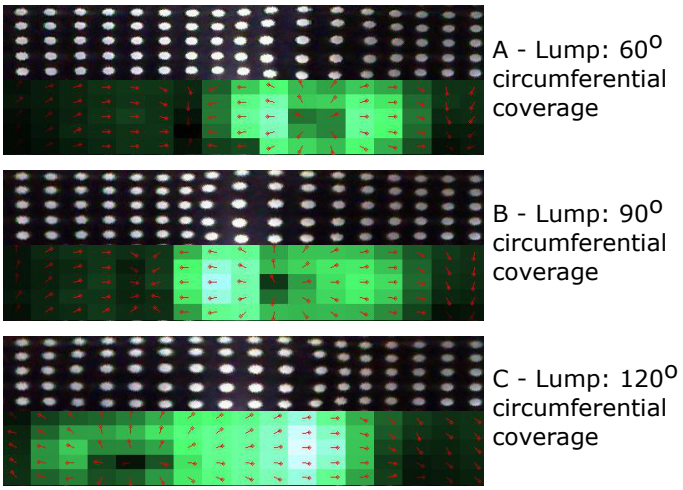

Fig. 9. Examples of contact with each of the three lump sizes. The unwrapped captured image sits above the visual representation of captured data. Each cell corresponds to one of the papillae pins, where its colour is determined by that pins vector magnitude. The angle of the vector is shown by the vector and marker layered above the cell.

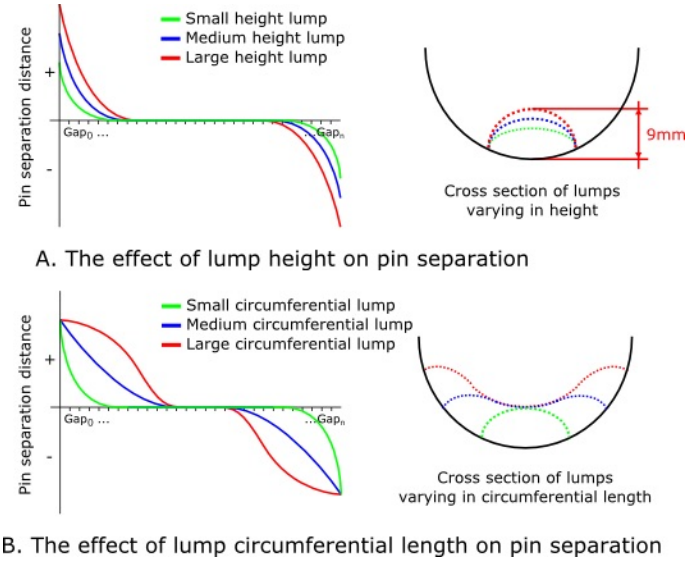

Fig. 10. Example of the effects of lump size and shape (as described in Fig. 13) on sensor data used as input to classifier system.

It is a non-probabilistic binary linear classifier that ring-fences results in to a strict type of category. An alternative is a multilayer perceptron Classifier Neural Network (CNN). A CNN is a feedforward artificial neural network model which can provide confidence based decision output rather than the explicit binary classification output of the SVM. This may be more useful within the context of tumour classification considering the variance found in natural tumorous growths. Whilst SVMs are less prone to over fitting, they are non-parametric models, meaning their size can increase with the size of the training set. A CNN however is a parametric model, so its size is fixed. This could be a consideration for a system that may constantly update itself with new patient information. Results of the two methods will be compared with the same input data.

In order to simplify the classification process, the data is sorted such that the values range from maximum to minimum. In doing so the radial position of the focal point of contact is lost from the data. However, this information is available through simpler means than a classifier, and bears little relivence to the classification of the lump. In its sorted form the data can be plotted, where the changes in the plot shape due to lump type would be as shown in Figure 10. In summary, with lumps of larger height the indentation of the sensor is greater so the maximum pin separation increases. Current experiments have only explored classification of one lump at one time, although with further training of the classifier using more complex lump scenarios identification of multiple lumps would be possible.

Fig. 11 shows two graphs, the first a general representation of average pin displacement against applied force for each test lump, both hard and soft. The second shows the individual pin displacement of the middle of pins at varying forces applied to the large hard 120^o test lump. Both graphs show the sensitivity of the sensor even at low forces, and also the shape characteristics detectable by the sensor. Whilst these experiments have used classifier groups that start to detect the presence of a lump 25% coverage in order to reduce complexity of input for the classifier, these graphs show promise for detection of much finer features at low forces.

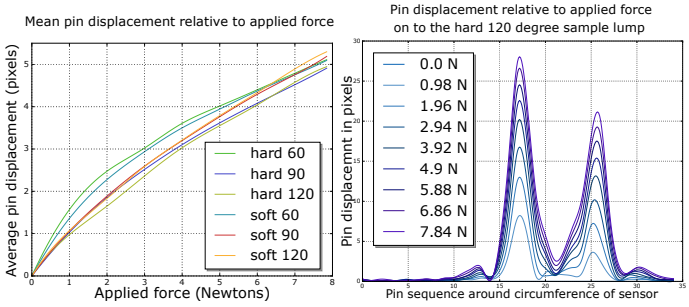

Fig. 11. The left figure presents the mean pin displacement of the middle three rows when pressed against each of the test lumps with a known force. The right figure shows individual pin displacement of the middle row of pins when subjected to a known force on to the hard 120^o test lump.

IV. Results

A. Lump detection

Considering the restrictions of size on capsule endoscopy, the power density of available power sources is limiting on capsule payload of onboard camera and computation. This presents a motivation to reduce both camera and computation in order to reduce the load of any onboard power source. The following experiments first investigate whether observation of simply the middle row of pins is sufficient for detection of lumps, and later explore the trade off of accuracy against computation complexity.

This article has been accepted for publication in a future issue of this journal, but has not been fully edited. Content may change prior to final publication. Citation information: DOI 10.1109/JSEN.2016.2627798, IEEE Sensors Journal

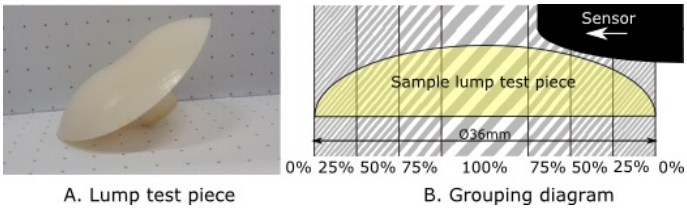

Fig. 12. A. 3D printed lump test piece used for lump detection experiment. B. Diagram showing how samples are grouped in relation to sample coverage and central position of sensor.

The first experiment tests whether a classifier system can detect whether a lump is present and by how much that lump is covered by the sensor. A binary classifier cannot provide confidence with results as a measure of how much a lump is present, so the samples are grouped in to regions of 0.0%, 25.0%, 50.0%, 75.0% and 100.0% lump coverage, see Fig. 12.B. A sample set of 2520 has been used which is randomised and split 50/50 between training and test data. This data is fed in to both a SVM and CNN classifiers and Table I presents the results and precision of both. The CNN is capable of providing confidence data and so the average confidence for the CNN is shown in the table. The results show a positive ability to detect the presence of a lump. Focus should be paid to 100% coverage detection rather than partial detection as this is where the lump is fully covered by the sensing envelope. In this case more than 90% accuracy can be achieved using the SVM and more than 80% with the CNN. Detection of no lump has greater success, but there are clear strengths in 'lump' / 'no lump' scenario. Results with partial detection where the sensor covers 25-75% of the lump are less positive but still achieve around the 70% region. These results show a clear ability to detect lump presence and the ability to classify to what extent a lump has been covered. Additionally the average confidence provided by the CNN shows the average confidence in the output class in all results.

TABLE I. LUMP DETECTION SVM AND CNN PRECISION RESULTS

Coverage/Group	SVM precision	CNN precision
0%	0.97	0.97
25%	0.74	0.59
50%	0.70	0.77
75%	0.69	0.70
100%	0.93	0.83
Ave / Total:	0.81	0.77
Ave confidence:	N/A	0.79

B. Lump size

Typically a submucosal tumour will begin to form on one region of the intestinal wall and spread around that wall circumferentially. In order to detect this the sensor will need to discriminate between the spread of deformed pins around the circumference as shown in Fig. 10.B. Fig. 13 shows the 3D printed hard test lumps varying in circumferential length. In this experiment three test pieces are used as apposed to the previous one. This increases the number of classifier groups from five to thirteen. The same principle of lump coverage is used in combination with lumps that cover $60^o, 90^o$ and 120^o of the sensor circumference. The additional test pieces increase the number of samples acquired to 7560. Again data is fed in to both a SVM and CNN classifiers and Table II presents the results and precision of both.

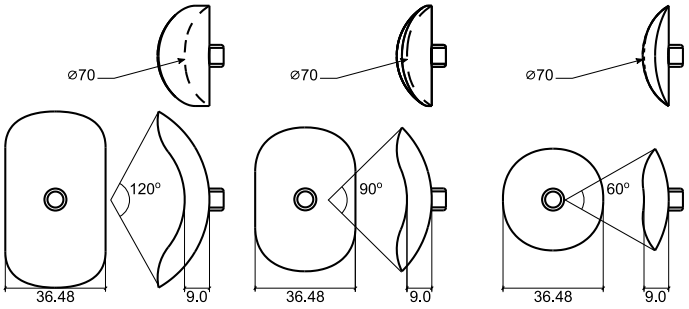

Fig. 13. Test pieces range in circumferential spread around the pipe, $120^o, 90^o$ and 60^o left to right. Test pieces are in two forms, solid and soft shore 15 silicone.

The results show little negative effect on the classifier detection rates for both SVM and CNN. This suggests that the classifier has potential for the ability to further discriminate sensor readings with more complex features. As with the previous lump detection experiment, the SVM leads the CNN with accuracy. There is a small increase in CNN average confidence but this is too small to be considered an improvement.

C. Lump hardness

Fig. 14. Soft test pieces spread circumferentially around sensor, $60^o, 90^o$ and 120^o left to right. Soft lumps are made from cast Platsil 7315 rubber silicone.

The final aim of this work is to discriminate between hard and soft tissue. Three new test pieces have been made the same shape and size as the previous circumferential length test pieces, only the new pieces are made using a shore 15 silicone, see Fig. 14. This forms a soft and deformable surface that will create a different interaction with the sensor compared to a rigid material test piece. These differences will be relatively small compared to the previous experiments so it is expected that the accuracy of the classifiers will decrease. Table II shows both the first results for classification of hard and soft lumps in combination with varying circumferential length and the second optimised results explained in the next section. The first

This article has been accepted for publication in a future issue of this journal, but has not been fully edited. Content may change prior to final publication. Citation information: DOI 10.1109/JSEN.2016.2627798, IEEE Sensors Journal

section of the table shows the results when only the middle row of pin data is used as an input for the classifier, the same input as the previous experiments. The results show a decline in accuracy of 3 and 5 percent for the SCV and CNN respectively from the previous size discrimination experiment. Table III isolates the grouping to hard or soft, in which the results are complimentary of Table II. The next section details efforts to improve accuracy by increasing the level of detail in the classifier input format.

TABLE II. HARDNESS SHAPE DETECTION SVM AND CNN PRECISION RESULTS

	Input: 1 row		Input: 3 rows	
Coverage/Group	SVM precision	CNN precision	SVM precision	CNN precision
0%	0.91	0.90	0.97	0.95
Hard−60°25%	0.41	0.28	0.77	0.79
Hard−60°50%	0.61	0.66	0.80	0.53
Hard−60°75%	0.76	0.57	0.88	0.50
Hard−60°100%	0.95	0.90	0.98	0.76
Hard−90°25%	0.57	0.52	0.79	0.74
Hard−90°50%	0.71	0.68	0.75	0.50
Hard−90°75%	0.86	0.86	0.88	0.44
Hard−90°100%	0.98	0.70	0.94	0.84
Hard−120°25%	0.64	0.44	0.84	0.81
Hard−120°50%	0.57	0.43	0.80	0.52
Hard−120°75%	0.86	0.73	0.88	0.51
Hard−120°100%	0.97	0.82	0.95	0.81
Soft-60°25%	0.41	0.19	0.82	0.72
Soft-60°50%	0.45	0.32	0.84	0.53
Soft-60°75%	0.62	0.35	0.87	0.52
Soft-60°100%	0.80	0.78	0.80	0.65
Soft-90°25%	0.46	0.41	0.68	0.63
Soft-90°50%	0.50	0.40	0.73	0.51
Soft-90°75%	0.54	0.53	0.73	0.47
Soft-90°100%	0.80	0.42	0.84	0.66
Soft-120°25%	0.70	0.54	0.66	0.69
Soft-120°50%	0.75	0.57	0.77	0.65
Soft-120°75%	0.85	0.58	0.80	0.53
Soft-120°100%	0.92	0.78	0.90	0.80
Ave / Total:	0.81	0.73	0.90	0.79
Ave confidence:	N/A	0.70	N/A	0.76

TABLE III. HARDNESS DETECTION SVM AND CNN PRECISION RESULTS

	Input: 1 row		Input: 3 rows	
Coverage/Group	SVM precision	CNN precision	SVM precision	CNN precision
Hard	0.78	0.78	1.00	1.00
Soft	0.71	0.63	1.00	0.99
Ave confidence:	N/A	0.69	N/A	0.99

D. Optimisation

The previous experiments have used a simplified classifier input of the middle row of pins only. This has been sufficient for discrimination to this point however the success and accuracy discriminating size and density has declined. In an attempt to increase accuracy, more data has been included in the input data that incorporates the row of pins above and below the middle row currently used. These three rows are separately sorted maximum to minimum as shown in Fig. 15, where the input is a list of values from the three rows of thirty five pins each. The second sections of Tables II and III detail the benefits of this increased data. By using three times the data the average accuracy has increased by almost 10 percent in the SVM and 6 percent in the CNN. When considering lump density on its own accuracy reaches 100 percent and 99 percent respectively. The increased data has a clearly positive effect on the accuracy of the classifier systems.

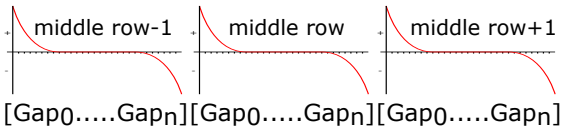

Fig. 15. Visualisation of the optimised classifier input data format. The new format consists of the pin delta values for the middle row of pins and one row above and below. Each row's data is kept seperate but they are concatenated together to form a 135 element long array. As with the previous experiment, each row's data is sorted from maximum to minimum values.

V. CONCLUSION

This publication has built upon the cylindrical Tactip design presented previously, [25]. Whilst this previous publication showed the principles in building the device and basic functionality towards deformation sensing, this publication has used learning systems to abstract the sensor data and classify different kinds of synthetic tumours based around the development of submucosal tumours. We have explored our hypothesis by collecting sample data of the cylindrical Tactip in contact with a variety of tumour like lumps and presenting the data to a classifier system. This has confirmed that the cylindrical Tactip is capable of discriminating between size, shape and density, all characteristics which determine the risk of a tumour. When the complexity of the classifier grouping increased with the introduction of different density lumps the accuracy of the classifier decreased, but this was easily countered with a more complex data format passed to the classifier which improved accuracy to a more acceptable average of 90%. This is a promising start towards achieving a remote palpation system used inside the GI tract that will help return the use of one of surgeon's most important skills their highly enhanced sense of touch.

This publication has presented a new application for a biologically inspired tactile sensing device. Whilst first thoughts of applications of the Tactip lead toward replication of typical fingertip type activities, we have proposed a new method of medical diagnostics. With the use of new 3D printing technology it has been possible to develop and prove this system quickly. Whilst the environment used to test the hypothesis is not typical to a human digestive tract, it is a step towards it. Future work with this device would expect further progress towards a more realistic digestive tract environment using compliant lumen like surfaces. There are two clear directions for future work. The cylindrical Tactip device is to be integrated with a suitable locomotion mechanism to move through the GI tract. There are many examples of robots capable of traveling through both rigid and compliant tube like structures that could be compatible with the Tactip such as

[35], [36], [37] or [13]. The second development should create a soft flexible environment which is more akin to the human GI tract which is soft, flexible and compliant. This would further increase the complexity and noise in the data obtained from the sensor which may cause the sensor to need a higher resolution of papillae pins, or additional surface features as explored by Winstone et al. [31] to amplify miniature contact features.

VI. Acknowledgment

Bristol Robotics Laboratory gratefully acknowledge that this work was supported by the Above & Beyond charity, http://www.aboveandbeyond.org.uk/.

References

[1] A. L. Trejos, J. Jayender, M. Perri, M. Naish, R. Patel, and R. Malthaner, "Robot-assisted Tactile Sensing for Minimally Invasive Tumor Localization," *The International Journal of Robotics Research*, vol. 28, no. 9, pp. 1118–1133, 2009.

[2] S. Schostek, C.-N. Ho, D. Kalanovic, and M. O. Schurr, "Artificial tactile sensing in minimally invasive surgery - a new technical approach.," *Minimally invasive therapy & allied technologies : MITAT : official journal of the Society for Minimally Invasive Therapy*, vol. 15, pp. 296–304, jan 2006.

[3] C. Roke, a. Spiers, T. Pipe, and C. Melhuish, "The effects of laterotactile information on lump localization through a teletaction system," *2013 World Haptics Conference (WHC)*, pp. 365–370, apr 2013.

[4] J. C. Gwilliam, Z. Pezzementi, E. Jantho, A. M. Okamura, and S. Hsiao, "Human vs. robotic tactile sensing: Detecting lumps in soft tissue," *2010 IEEE Haptics Symposium*, pp. 21–28, mar 2010.

[5] A. P. Sarvazyan, "Computerized palpation is more sensitive than human finger.," in *Proceedings of the 12th International Symposium on Biomedical Measurements and Instrumentation.*, pp. 523–24, 1998.

[6] A. Menciassi, M. Quirini, and P. Dario, "Microrobotics for future gastrointestinal endoscopy.," *Minimally invasive therapy & allied technologies : MITAT : official journal of the Society for Minimally Invasive Therapy*, vol. 16, pp. 91–100, jan 2007.

[7] S. Dogramadzi, G. S. Virk, G. D. Bell, R. S. Rowland, and J. Hancock, "Recording forces exerted on the bowel wall during colonoscopy: in vitro evaluation.," *The international journal of medical robotics + computer assisted surgery : MRCAS*, vol. 1, pp. 89–97, dec 2005.

[8] K. Rebello, "Applications of MEMS in Surgery," *Proceedings of the IEEE*, vol. 92, pp. 43–55, jan 2004.

[9] K. Kume, T. Kuroki, T. Sugihara, and M. Shinngai, "Development of a novel endoscopic manipulation system: The Endoscopic operation robot.," *World journal of gastrointestinal endoscopy*, vol. 3, pp. 145–50, jul 2011.

[10] A. Chaudhary, D. Atal, and S. Kumar, "Robotic Surgical SystemsA Review," *International Journal of Applied . . .*, vol. 9, no. 11, pp. 1289–1294, 2014.

[11] M. E. Rentschier, J. Dumpert, S. R. Platt, D. Oleynikov, S. M. Farritor, and K. Iagnemma, "Mobile in vivo biopsy robot," *Proceedings - IEEE International Conference on Robotics and Automation*, vol. 2006, no. May, pp. 4155–4160, 2006.

[12] S. Park, H. Park, and B. Kim, "A paddling based locomotive mechanism for capsule endoscopes," *Journal of mechanical science and technology (KSME Int. J.)*, vol. 20, no. 7, pp. 1012–1018, 2006.

[13] M. Quirini and S. Scapellato, "An approach to capsular endoscopy with active motion," *IEEE EMBS*, vol. 29, pp. 2827–30, jan 2007.

[14] S. P. Woods and T. G. Constandinou, "Towards a micropositioning system for targeted drug delivery in wireless capsule endoscopy.," *IEEE Engineering in Medicine and Biology Society. Conference*, vol. 2011, pp. 7372–5, jan 2011.

[15] N. H. Cox and J. R. Soc, "Palpation of the skin, an important issue," *Journal of the Royal Society of Medicine*, vol. 99, pp. 598–601, jan 2006.

[16] J. Konstantinova, A. Jiang, K. Althoefer, P. Dasgupta, and T. Nanayakkara, "Implementation of tactile sensing for palpation in robot-assisted minimally invasive surgery: A review," *IEEE Sensors Journal*, vol. 14, no. 8, pp. 2490–2501, 2014.

[17] J. Dargahi and S. Najarian, "Human tactile perception as a standard for artificial tactile sensing - a review," *International Journal of Medical Robotics and Computer Assisted Surgery*, vol. 01, no. 01, p. 23, 2004.

[18] A. P. Åstrand, V. Jalkanen, B. M. Andersson, and O. A. Lindahl, "Detection of Stiff Nodules Embedded in Soft Tissue Phantoms , Mimicking Cancer Tumours , Using a Tactile Resonance Sensor," *Journal of Biomedical Science and Engineering*, no. March, pp. 181–193, 2014.

[19] M. Nyberg, V. Jalkanen, K. Ramser, B. Ljungberg, a. Bergh, and O. a. Lindahl, "Dual-modality probe intended for prostate cancer detection combining Raman spectroscopy and tactile resonance technology–discrimination of normal human prostate tissues ex vivo," *J Med Eng Technol*, vol. 39, no. 3, pp. 198–207, 2015.

[20] C. Chuang, Yung-Kang, T. Li, I. Chou, and Y. Teng, "Piezoelectric tactile sensor for submucosal tumor hardness detection in endoscopy," in *Solid-State Sensors, Actuators and Microsystems (TRANSDUCERS), 2015 Transducers - 2015 18th International Conference on*, pp. 871–875, IEEE, 2015.

[21] A. Talasaz and R. V. Patel, "Integration of force reflection with tactile sensing for minimally invasive robotics-assisted tumor localization," *IEEE Transactions on Haptics*, vol. 6, no. 2, pp. 217–228, 2013.

[22] Y. Tanaka, M. Fujiware, and A. Sano, "Lump detection with tactile sensing system including haptic bidirectionality," in *World Automation Congress (WAC), 2014*, pp. 1–6, 2014.

[23] G. Ciuti, R. Caliò, D. Camboni, L. Neri, F. Bianchi, A. Arezzo, A. Koulaouzidis, S. Schostek, D. Stoyanov, C. M. Oddo, B. Magnani, A. Menciassi, M. Morino, M. O. Schurr, and P. Dario, "Frontiers of robotic endoscopic capsules: a review," *Journal of Micro-Bio Robotics*, 2016.

[24] Q. Shi, J. Wang, D. Chen, J. Chen, J. Li, and K. Bao, "In Vitro and In Vivo characterization of wireless and passive micro system enabling gastrointestinal pressure monitoring.," *Biomedical Microdevices*, vol. 16, pp. 859–68, aug 2014.

[25] B. Winstone, "Biomimetic Tactile Sensing Capsule," in *Living Machines*, (Barcelona), pp. 113–122, Springer, 2015.

[26] T. Assaf, C. Chorley, J. Rossiter, T. Pipe, C. Stefanini, and C. Melhuish, "Realtime Processing of a Biologically Inspired Tactile Sensor for Edge Following and Shape Recognition," *TAROS*, 2010.

[27] B. Winstone, C. Melhuish, and S. Dogramadzi, "A Novel Bio-inspired Tactile Tumour Detection Concept for Capsule Endoscopy," in *Biomimetic and Biohybrid Systems: Third International Conference, Living Machines*, pp. 442–5, 2014.

[28] M. Kamba, Y. Seta, A. Kusai, M. Ikeda, and K. Nishimura, "A unique dosage form to evaluate the mechanical destructive force in the gastrointestinal tract," *International Journal of Pharmaceutics*, vol. 208, no. 1-2, pp. 61–70, 2000.

[29] B. Winstone, G. Griffiths, C. Melhuish, and T. Pipe, "TACTIP - Tactile Fingertip Device , Challenges in reduction of size to ready for robot hand integration," in *IEEE Robotics and Biomimetics (ROBIO)*, (Guangzhou), pp. 160–166, 2012.

[30] a. B. Vallbo and R. S. Johansson, "Properties of cutaneous mechanoreceptors in the human hand related to touch sensation.," *Human neurobiology*, vol. 3, no. 1, pp. 3–14, 1984.

[31] B. Winstone, G. Griffiths, T. Pipe, and J. Rossiter, "TACTIP - Tactile Fingertip Device , Texture Analysis Through Optical Tracking of Skin Features," in *Biomimetic and Biohybrid Systems: Third International Conference, Living Machines*, 2013.

[32] M. Arian and C. Blaine, "Using the BioTac as a tumor localization tool," *IEEE Haptics Symposium*, pp. 443–448, 2014.

[33] S. Mckinley, A. Garg, S. Sen, D. V. Gealy, J. P. Mckinley, Y. Jen, and K. Goldberg, "Autonomous Multilateral Surgical Tumor Resection with Interchangeable Instrument Mounts and Fluid Injection Device," in *IEEE ICRA*, 2016.

[34] J. WorsØe, L. Fynne, T. Gregersen, V. Schlageter, L. a. Christensen, J. F. Dahlerup, N. J. Rijkhoff, S. Laurberg, and K. Krogh, "Gastric transit and small intestinal transit time and motility assessed by a magnet tracking system," *BMC Gastroenterology*, vol. 11, no. 1, p. 145, 2011.

[35] A. Boxerbaum and A. Horchler, "Worms, waves and robots," in *IEEE ICRA*, pp. 3537–3538, 2012.

[36] A. Horchler, A. Kandhari, K. Daltorio, K. Moses, K. Andersen, H. Bunnelle, J. Kershaw, W. Tavel, H. Chiel, R. Bachmann, and R. Quinn, "Worm-Like Robotic Locomotion with a Compliant Modular Mesh," in *Biomimetic and Biohybrid Systems* (S. P. Wilson, P. F. Verschure, A. Mura, and T. J. Prescott, eds.), vol. 9222 of *Lecture Notes in Computer Science*, (Barcelona), pp. 26–37, Springer International Publishing, 2015.

[37] S. Seok, C. D. Onal, K.-J. Cho, R. J. Wood, D. Rus, and S. Kim, "Meshworm: A Peristaltic Soft Robot With Antagonistic Nickel Titanium Coil Actuators," *IEEE/ASME Transactions on Mechatronics*, vol. 18, pp. 1485–1497, oct 2013.